Inorg. Chem. **2008**, *47*, 11644−11655

Large Amplitude, Proton- and Cation-Activated Latch-Type Mechanical Switches: O-Protonated Amides Stabilized by *Intramolecular*, Low-Barrier Hydrogen Bonds within Macrocycles

Mariappan Kadarkaraisamy,[†] Gerald Caple,[†] Andrea R. Gorden,[†] Marie A. Squire,[‡] and Andrew G. Sykes*,[†]

Department of Chemistry, University of South Dakota, Vermillion, South Dakota 57069, and Department of Chemistry, University of Canterbury, Christchurch 8140, New Zealand

Received July 7, 2008

Large amplitude molecular switches have been developed using oxonium ions as the novel switching mechanism. Macrocycles that contain a polyether ring that are preorganized and of optimum geometry such that strong, linear Low-Barrier Hydrogen Bonds (LBHB, 2.4 to 2.6 Å in length) are formed between a protonated amide oxygen and a cyclic ether, that lend significant iminol character to the amide. Deprotonation yields a large conformational change between closed and open forms, mindful of a new hinged, latch-type mechanical proton switch. Numerous open and closed forms have been characterized by X-ray crystallography, and the intramolecular hydrogen bond that forms between the protonated amide oxygen and the cyclic polyether oxygen accounts for the stability of these new acids. The open form of the deprotonated adducts persist in solution as indicated by the magnitude of coupling constants and other Nuclear Overhauser Effect experiments. Different saturated and unsaturated solid acids have been characterized including products derived from acetonitrile, propionitrile, caprylonitrile, acrylonitrile and adiponitrile, and also by reaction with primary amides in the case of phenyl and norbornene derivatives. We have also demonstrated that metal cations can replace the proton in the switching mechanism, characteristic of nascent synthetic pores.

Introduction

In this report, a Lewis-acid activated mechanical switch with a closing latch-type mechanism is produced via (A) protonated oxonium ions stabilized by an *intramolecular* hydrogen bond that forms between an O-protonated amide and a macrocyclic ether oxygen, $HNC{=}O^{+}{-}H\cdots OR_2$, and (B) complexation with a metal cation of the same motif (Scheme 1). Proton switches in their most recognizable guise are colorimetric and/or fluorometric sensors where the presence (or absence) of a Lewis acid changes the electronic state of the chromophore/lumophore. These sensors have been previously reviewed and include our own work in this area.[1,2] Proton switches that incur large amplitude changes in physical structure are far less common, however. These switches are of the mechanical type, implying movement with the eventual goal of prescribed motion involving molecular machines. Mechanical switches utilizing protons as the switching mechanism, up to now, have also included the absorption of a photon in the case of reversible ring opening and closing in benzspiropyrans and diarylethene compounds;[3] the translocation of metal cations between adjacent binding sites upon change in pH;[4] or changes in conformation because of solvent polarity, including chair-

* To whom correspondence should be addressed. E-mail: asykes@usd.edu.
[†] University of South Dakota.
[‡] University of Canterbury.

(1) (a) *Fluorescent Chemosensors for Ion and Molecular Recognition*; Czarnik, A.W., Ed.; American Chemical Society: Washington, DC, 1992. (b) Bissell, R. A.; de Silva, A. P.; Gunaratne, H. Q. N.; Lynch, P. L. M.; Maguire, G. E. M.; Sandanayake, K. R. A. S. *Chem. Soc. Rev.* **1992**, 187. (c) de Silva, A. P.; Gunaratne, H. Q. N.; Gunnlaugsson, T.; Huxley, A. J. M.; McCoy, C. P.; Rademacher, J. T.; Rice, T. E. *Chem. Rev.* **1997**, *97*, 1515. (d) Rurack, K. *Spectrochim. Acta* **2001**, *A57*, 2161. (e) Prodi, L. *New. J. Chem.* **2005**, *29*, 20.

(2) (a) Young, V. G., Jr.; Quiring, H. L.; Sykes, A. G. *J. Am. Chem. Soc.* **1997**, *119*, 12477–12480. (b) Kampmann, B.; Lian, Y.; Klinkel, K. L.; Vecchi, P. A.; Quiring, H. L.; Soh, C. C.; Sykes, A. G. *J. Org. Chem.* **2002**, *67* (11), 3878–3883. (c) Kadarkaraisamy, M.; Dufek, E.; LoneElk, D.; Sykes, A. G. *Tetrahedron* **2005**, *61*, 479. (d) Kadarkaraisamy, M.; Sykes, A. G. *Inorg. Chem.* **2006**, *45*, 779. (e) Liu, Z.; Sykes, A. G. *J. Chem. Crystallogr.* **2006**, *36*, 875. (f) Kadarkaraisamy, M.; Sykes, A. G. *Polyhedron* **2007**, *26*, 1323.

10.1021/ic801238a CCC: $40.75
Published on Web 11/13/2008

Scheme 1

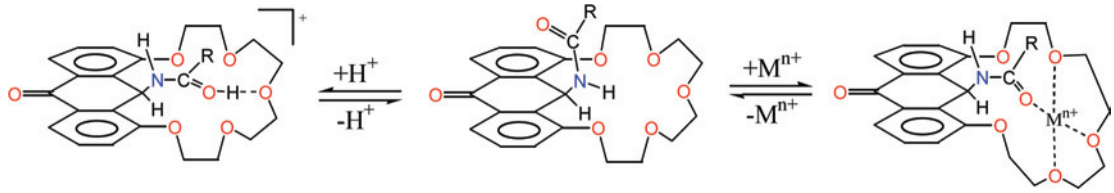

boat and E-Z isomerization.[5] Mechanical proton switches have also been observed altering the host−guest chemistry of ditopic macrocycles[6] and rotaxanes[7] and also produce conformation changes in large DNA adducts.[8] None of these examples involve as large of an amplitude change in geometry as observed in this case, however.

O-protonated amides have previously been characterized by crystallographic methods and exist in two forms: (1) protonated amides hydrogen-bonded directly to the conjugate base of a strong mineral acid, that is, C=O$^+$−H···A$^-$[9] and (2) hemiprotonated dimers of amides with C=O···H···O=C bridges.[10] All of these cases involve formation of *intermolecular* hydrogen bonds. To our knowledge, only two examples exist involving *intramolecular* hydrogen bond formation of O-protonated amides. A protonated primary amide-tetracycline derivative contains a short, bent (∼130°) hydrogen bond,[11] similar to nonamide related hydrogen-bonding observed in protonated benzolyacetones (containing a *cis*-β-keto−enol structure).[12] A second example involves intramolecular hydrogen bonding across a macrocyclic ring structure forming a hemiprotonated diamide (HNC=O···H$^+$···O=CNH).[13] Because of large differences in pK_a, protonation of amide carbonyl oxygens (pK_a = ∼0) almost always occur over protonation of the amide nitrogen (∼−7), with the exception of Lectka's amide proton sponge, where the hydrogen bond forms between the amide nitrogen and the immediately adjacent protonated amine group.[14]

Scheme 2

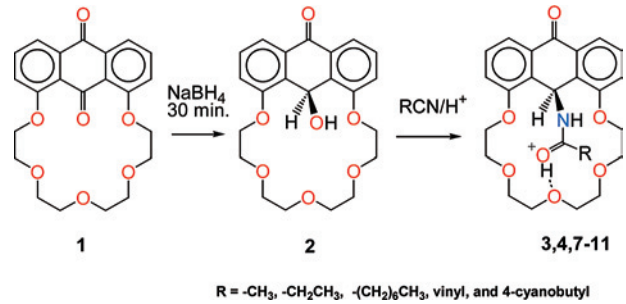

We have employed the Ritter amide synthesis to produce solid acids by combining a secondary alcohol with both nitriles or primary amides in the presence of acid (Scheme 2).[15] Benzhydrol (diphenylmethanol), similar to **2**, is also a secondary alcohol used in the synthesis of amides, where the aromatic rings stabilize the incipient carbocation formed during the reaction.[16] The Ritter synthesis is a relatively uncommon method for the production of amides, however, but allows for significant synthetic versatility as commercially available nitriles can be readily substituted. In this fashion,

(3) (a) Kawai, S. H.; Gilat, S. L.; Lehn, J. M. *Eur. J. Org. Chem.* **1999**, 2359. (b) Raymo, F. M.; Giordani, S. *Org. Lett.* **2001**, *3*, 3475. (c) Guo, X.; Zhang, D.; Zhou, Y.; Zhu, D. *Chem. Phys. Lett.* **2003**, *375*, 484. (d) Giordani, S.; Cejas, M. A.; Raymo, F. M. *Tetrahedron* **2004**, *60*, 10973.

(4) (a) Amendola, V.; Fabbrizzi, L.; Mangano, C.; Pallavicini, P.; Perotti, A.; Tagletti, A. *J. Chem. Soc., Dalton Trans.* **2000**, 183. (b) Ambrossi, G.; Dapportp, P.; Formica, M.; Fusi, V.; Giorgi, L.; Guerri, A.; Micheloni, M.; Paoli, P.; Pontellini, R.; Rossi, P. *Chem.—Eur. J.* **2003**, *9*, 800. (c) Liu, H. J.; Hung, Y. H.; Chou, C. C.; Su, C. C. *Chem. Commun.* **2007**, 495.

(5) (a) Perez, E. M.; Dryden, D. T. F.; Leigh, D. A.; Teobaldi, G.; Zerbetto, F. *J. Am. Chem. Soc.* **2004**, *126*, 12210. (b) Onoda, A.; Haruna, H.; Yamamoto, H.; Takahashi, K.; Kozuki, H.; Okamura, T.; Ueyama, N. *Eur. J. Org. Chem.* **2005**, 641.

(6) (a) Jones, J. W.; Bryant, W. S.; Bosman, A. W.; Janssen, R. A. J.; Meijer, E. W.; Gibson, H. W. *J. Org. Chem.* **2003**, *68*, 2385. (b) Huang, F.; Switek, K. A.; Gibson, H. W. *Chem. Commun.* **2005**, 3655. (c) Yen, M. L.; Li, W. S.; Lai, C. C.; Chao, I.; Chiu, S. H. *Org. Lett.* **2006**, *8*, 3223.

(7) (a) Lee, J. W.; Kim, K.; Kim, K. *Chem. Commun.* **2001**, 1042. (b) Elizarov, A. M.; Chiu, S. H.; Stoddart, J. F. *J. Org. Chem.* **2002**, *67*, 9175. (c) Badjic, J. D.; Balzani, V.; Credi, A.; Silvi, S.; Stoddart, J. F. *Science* **2004**, *303*, 1845.

(8) Liedl, T.; Simmel, F. C. *Nano Lett.* **2005**, *5*, 1894.

(9) (a) Winkler, F. K.; Dunitz, J. D. *Acta Crystallogr. B* **1975**, *31*, 278–281. (b) Winkler, F. K.; Dunitz, J. D. *Acta Crystallogr. B* **1975**, *31*, 273–275. (c) Kildea, J. D.; White, A. H. *Inorg. Chem.* **1984**, *23*, 3825–27. (d) Calabrese, J. C.; Gardner, K. H. *Acta Crystallogr. C* **1985**, *41*, 389–392. (e) Tsang, K. Y.; Diaz, H.; Graciani, N.; Kelly, J. W. *J. Am. Chem. Soc.* **1994**, *116*, 3988. (f) Escudero, E.; Subirana, J. A.; Solans, X. *Acta Crystallogr. C* **1999**, *55*, 644–646. (g) Chin, C. S.; Chong, D.; Lee, B.; Jeong, H.; Won, G.; Do, Y.; Park, Y. J. *Organometallics* **2000**, *19*, 638–648. (h) Nagao, H.; Hirano, T.; Naotoshi, T.; Shiota, S.; Mukaida, M.; Oi, T.; Yamasaki, M. *Inorg. Chem.* **2002**, *41*, 6267–6273. (i) Shine, H. J.; Zhao, B. J.; Marx, J. N.; OuldEly, T.; Whitmire, K. H. *J. Org. Chem.* **2004**, *69*, 9255–9261.

(10) (a) Hussein, M. S.; Schlemper, E. O. *J. Chem. Soc., Dalton Trans.* **1980**, 750–55. (b) Gubin, A. I.; Yanovsky, A. I.; Struchkov, Y. T.; Nurakhunelov, N. N.; Baranbaev, M. Z.; Beremzhanov, B. A. *Izv. Akad. Nauk Kaz. SSR, Ser. Khim* **1986**, 78–86. (c) Gubin, A. I.; Baranchbaev, M. Z.; Kostynyuk, V. P.; Kopot, O. J.; Irin, A. I. *Krystallografiya* **1988**, *33*, 1393–1395. (d) Hill, C. L.; Bouchard, D. A.; Kadkhodayan, M.; Williamson, M. M.; Schmidt, J. A.; Hilinski, E. F. *J. Am. Chem. Soc.* **1988**, *110*, 5471–5479. (e) Gubin, A. I.; Baranbaev, M. Z.; Erleansov, R. S.; Nurakhunelov, N. N.; Khakimzhanova, G. D. *Kristallografiya* **1989**, *34*, 1305–1306. (f) Suh, M. P.; Oh, K. Y.; Lee, J. W.; Bae, Y. Y. *J. Am. Chem. Soc.* **1996**, *118*, 777–783. (g) Krill, J.; Shevchenko, I. V.; Fisher, A.; Jones, P. G.; Schmutzler, R. *Chem. Ber.* **1997**, *130*, 1479–1483. (h) Wilhelm, M.; Koch, R.; Strasdeit, H. *New J. Chem.* **2002**, *26*, 560–566. (i) Suzuki, H.; Ishiguro, S. *Acta Crystallogr. E* **2006**, *62*, m576–578.

(11) Stezowski, J. *J. Am. Chem. Soc.* **1977**, *99*, 1122.

(12) Schiøtt, B.; Iverson, B. B.; Madsen, G. K. H.; Larsen, F. K.; Bruice, T. C. *Proc. Natl. Acad. Sci. U.S.A.* **1998**, *95*, 12799–12802.

(13) Day, V. W.; Hossain, M. A.; Kang, S. O.; Powell, D.; Lushington, G.; Bowman-James, K. *J. Am. Chem. Soc.* **2007**, *129*, 8692–8693.

(14) Cox, C.; Wack, H.; Lectka, T. *Angew. Chem., Int. Ed.* **1999**, *38*, 798.

(15) (a) Ritter, R.; Minieri, P. P. *J. Am. Chem. Soc.* **1948**, *70*, 4045–48. (b) The Ritter Reaction, Krimin, L. I.; Cota, D. J. *Organic Reactions*; Krieger Publishing: Malabar, FL, 1969; pp 213−325.

a host of different solid acid analogues that incorporate a wide range of functional groups can be made. Short O−H···O hydrogen bond distances of ∼2.5 Å are observed, and we have characterized several saturated and unsaturated acid adducts.

Experimental Section

Reagents. 1,8-oxybis(ethyleneoxyethyleneoxy)anthracene-9,10-dione (**1**) was synthesized as previously reported.[17] Perchloric acid (70%), sodium borohydride (Aldrich), and nitriles (Aldrich) were purchased and used without purification. 5-norbornene-2-carboxamide (∼80:20 endo:exo) was purchased from Frinton Laboratories, Inc. CHN analyses were performed using a CE-440 (Exeter Analytical Inc.) elemental analyzer, and Electrospray Injection-Mass Spectroscopy was conducted using a Varian 500-MS IT Mass Spectrometer. Melting points were determined using an open capillary and are uncorrected. A Varian Mercury 200 was used to run NMR samples. The oxonium proton, H(99), was not observable in CD_3CN up to 20 ppm, and poor solubility prevented the use of other nonpolar solvents. **Caution!** *Although we have experienced no difficulties with these perchlorate salts, they should be regarded as potentially explosive and handled with care.*

Synthesis. 1,8-Oxybis(ethyleneoxyethyleneoxy)-10-hydroxy-10-hydro-anthracene-9-one (2). A 1.00 g quantity of **1** (2.5 mmol) was suspended in 50 mL of 95% ethanol and mixed with 0.095 g of sodium borohydride (2.5 mmol). The mixture was stirred for 30 min, poured into 100 mL of distilled water and extracted with methylene chloride (3 × 50 mL). The organic layer was dried over anhydrous sodium sulfate and purified by column chromatography using silica gel and methylene chloride. A tan amorphous powder was obtained. Yield: 0.80 g (∼80%) and melting point = 190−192 °C. Elemental analyses calcd for $C_{22}H_{24}O_7$: C, 65.99; H, 6.04%. Found: C, 65.78; H, 6.00%. ^{1}H NMR ($CDCl_3$, 22 °C): δ 3.67−3.89 (*m*, 12H, -CH_2O); 4.21−4.28 (*m*, 4H, -CH_2O); 6.36 (*s*, 1H, methine H); 7.09 (*d*, 8.2 Hz, 2H, ArH); 7.37 (*t*, 8.2 Hz, 2H, ArH); 7.83 (*d*, 7.8 Hz, 2H, ArH). ^{13}C NMR ($CDCl_3$, 22 °C): δ 56.3; 67.8; 68.9; 69.9; 70.6; 116.2; 119.4; 128.8; 132,0; 132.4; 156.6; 184.3.

1,8-Oxybis(ethyleneoxyethyleneoxy)-10-*N*-acetiminol-10-hydro-anthracene-9-one Perchlorate (3). A 0.25 g quantity (0.62 mmol) of **2** in 10 mL of acetonitrile was mixed with several drops of 70% perchloric acid and stirred. The yellow solution changed immediately to blue and faded to light brown after 10 min. The solution was slowly evaporated to give colorless crystals. Yield: 0.20 g (59%) and the melting point = 148−150 °C (dec). Elemental analyses calcd for $C_{24}H_{28}ClNO_{11}$: C, 53.19; H, 5.21; N, 2.58%. Found: C, 53.25; H, 5.16; N, 2.89%. ESI MS calcd for M^+: 442.48; Found: 442.19. ^{1}H NMR (CD_3CN at 22 °C): δ 2.21 (*s*, 3H, CH_3); 3.62−4.18 (*m*, 16H, -CH_2O); 6.49 (*d*, 9.4 Hz, 1H, methine H); 7.29 (*d*, 8.2 Hz, 2H, ArH); 7.58 (*t*, 7.8 Hz, 2H, ArH); 7.85 (*d*, 7.8 Hz, 2H, ArH); 8.36 (*d*, 9.4 Hz, 1H, NH). ^{13}C NMR (CD3CN at 22 °C): δ 20.6; 42.9; 68.6; 69.8; 70.8; 71.2; 125.7; 131.5; 133.3; 157.8; 182.2.

1,8-Oxybis(ethyleneoxyethyleneoxy)-10-*N*-ethyliminol-10-hydro-anthracene-9-one Perchlorate (4). A 0.20 g quantity (0.50 mmol) of **2** in 10 mL of propionitrile were combined in a similar manner as **3**. A pale yellow colored solid was obtained, filtered, washed several times with diethyl ether, and dissolved in acetonitrile/methanol (8:2) and diffused with diethyl ether. Colorless crystals were obtained. Yield: 0.12 g (∼53%) and the melting point = 168−171 °C (dec). Elemental analyses calcd for $C_{25}H_{30}ClNO_{11}$: C, 54.03; H, 5.44; N, 2.51%. Found: C, 54.65; H, 5.51; N, 2.20%. ESI MS calcd for M^+: 456.51; Found: 456.11. ^{1}H NMR (CD_3CN at 22 °C): δ 1.03 (*t*, 7.4 Hz, 3H, CH_3); 2.57 (*quartet*, 7.4 Hz, 2H, CH_2); 3.61−4.29 (*m*, 16H, -OCH_2); 6.62 (*d*, 9.4 Hz, 1H, methine H); 7.29 (*d*, 8.2 Hz, 2H, ArH); 7.59 (*t*, 8.2 Hz, 2H, ArH); 7.85 (*d*, 7.8 Hz, 2H, ArH); 8.23 (*d*, 9.4 Hz, 1H, NH). ^{13}C NMR (CD_3CN at 22 °C): δ 9.5; 28.3; 40.4; 8.7; 69.7; 70.8; 71.3; 116.6; 117.8; 128.5; 129.9; 133.8; 155.6; 181.2.

1,8-Oxybis(ethyleneoxyethyleneoxy)-10-*N*-ethylamido-10-hydro-anthracene-9-one Monohydrate (5). A 0.2 g quantity of **4** was suspended in 20 mL of distilled water. 20% aqueous sodium hydroxide was added until the solution became basic and was stirred for 1 h. The neutralized amide was extracted into methylene chloride, dried over sodium sulfate, and evaporated to dryness. The residue was dissolved in a 9:1 methylene chloride/methanol mixture and diffused with diethyl ether. A cream color crystalline solid was obtained. Yield 0.16 g (quantitative) and the melting point = 268−270 °C (dec). Elemental analyses calcd for $C_{25}H_{29}NO_7.H_2O$: C, 63.41; H, 6.60; N, 2.96%. Found: C, 63.35; H, 6.55; N, 3.18%. ^{1}H NMR (CD_3CN at 22 °C): δ 0.83 (*t*, 7.8 Hz, 3H, CH_3); 1.93 (*quartet*, 7.8 Hz, 2H, CH_2); 3.68−4.32 (*m*, 16H, -OCH_2); 5.77 (*d*, 7.0 Hz, 1H, methine H); 7.06 (*d*, 8.2 Hz, 2H, ArH); 7.36 (*t*, 7.8 Hz, 2H, ArH); 7.74 (*d*, 7.0 Hz, 1H, NH); 7.87 (*d*, 7.8 Hz, 2H, ArH). ^{13}C NMR (CD_3CN at 22 °C): δ 9.35; 29.1; 41.9; 68.1; 69.2 70.2; 70.4; 115.6; 119.3; 128.3; 129.8; 134.4; 155.5; 172.8; 184.3.

1,8-Oxybis(ethyleneoxyethyleneoxy)-10-*N*-benziminol-10-hydro-anthracene-9-one Perchlorate (6). A 0.2 g quantity (0.5 mmol) of **2** and 0.067 g (0.55 mmol) of benzamide were dissolved in 10 mL of benzonitrile. The above solution was mixed with three drops of 70% perchloric acid and stirred. The yellow solution changed immediately to blue and faded to light yellow after 10 min. The solution was stirred for half-hour and mixed with an excess of diethyl ether. A pale yellow solid was obtained, filtered and washed several times with diethyl ether. All solids were dissolved in a minimum amount of CH_3CN and diffused with diethyl ether. Pale yellow crystals were obtained. Yield: 0.21 g (70%) and the melting point = 152−156 °C (dec). Elemental analyses calcd for $C_{29}H_{30}ClNO_{11}$: C, 57.68; H, 5.00; N, 2.32%. Found: C, 57.66; H, 5.04; N, 2.39%. ESI MS calcd for M^+: 504.56; Found: 503.98. ^{1}H NMR (CD_3CN at 22 °C): δ 3.51−4.31 (*m*, 16H, -CH_2O); 6.70 (*d*, 9.0 Hz, 1H, methine H); 7.31 (*d*, 8.2 Hz, 2H, ArH); 7.42−7.68 (*m*, 7H, ArH); 7.84 (*d*, 7.8 Hz, 2H, ArH); 8.87 (*d*, 9.0 Hz, 1H, NH). ^{13}C NMR (CD_3CN at 22 °C): δ 43.4; 68.6; 69.8; 70.7; 70.8; 126.5; 128.8; 129.9; 131.4; 133.9; 134.6; 157.5; 171.5; 183.2.

1,8-Oxybis(ethyleneoxyethyleneoxy)-10-*N*-benzamido-10-hydro-anthracene-9-one (7). A 0.2 g quantity of **6** was neutralized in a manner similar to **5**. A cream color solid was obtained. Yield 0.17 g (quantitative) and the melting point = 228−232 °C (dec). Elemental analyses calcd for $C_{29}H_{29}NO_7.H_2O$: C, 66.78; H, 5.99; N, 2.69%. Found: C, 66.90; H, 5.86; N, 2.69%. NMR ($CDCl_3$ at 22 °C): δ 3.44−4.26 (*m*, 16H, -CH_2O); 6.04 (*d*, 7.0 Hz, 1H, methine H); 7.06 (*d*, 8.2 Hz, 2H, ArH); 7.25−7.33 (*m*, 3H, ArH); 7.38 (*t*, 7.8 Hz,

(16) (a) Kumar, B.; Kumar, H.; Singh, N. *Ind. J. Chem. B* **1991**, *30B*, 460–461. (b) Sampath, K.; Halmuthur, M.; Subba Reddy, B. A. *New J. Chem.* **1999**, *23*, 955–956. (c) Jain, N.; Krishnamuty, H. G. *Ind. J. Chem. B* **1999**, *38B*, 865–866. (d) Salehi, P.; Motlagh, A. R. *Synth. Commun.* **2000**, *30*, 671–675. (e) Salehi, P.; Khodaei, M. M.; Zolfigol, M. A.; Keyvan, A. *Synth. Commun.* **2001**, *31*, 1847–1951. (f) Gullickson, G. C.; Lewis, D. E. *Synthesis* **2003**, 681–684. (g) Gullickson, G. C.; Lewis, D. E. *Aust. J. Chem.* **2003**, *56*, 385–388. (h) Maki, T.; Ishihara, K.; Hisashi, Y. *Org. Lett.* **2006**, *8*, 1431–1434. (i) Fatemeh, T.; Khoobi, M.; Keshavarz, E. *Tetrahedron Lett.* **2007**, *48*, 3643–3646.

(17) Delgado, M.; Gustowski, D. A.; Yoo, H. K.; Gatto, V. J.; Gokel, G. W.; Echegoyen, L. *J. Am. Chem. Soc.* **1988**, *110*, 119.

2H ArH); 7.77 (*d*, 8.2 Hz, 2H, ArH); 7.91 (*d*, 8.2 Hz, 2H, ArH); 8.64 (*d*, 6.2 Hz, 1H, NH). ^{13}C NMR ($CDCl_3$ at 22 °C): δ 42.1; 67.8; 69.2; 70.2; 70.4; 115.2; 119.2; 127.6; 127.9; 128.4; 129.9; 131.4; 133.9; 156.5; 172.1; 182.5. Crystals were grown from 9:1 methylene chloride/methanol and diffused with diethyl ether.

(1,8-Oxybis(ethyleneoxyethyleneoxy)-10-*N*-acetamido-10-hydro-anthracene-9-one)lead(II) Perchlorate (8). Crystals were grown by the evaporation of a 1:1 mixture of base-neutralized **3** and $Pb(ClO_4)_2$ in acetonitrile. Elemental analyses calcd for $C_{24}H_{27}Cl_2NO_{15}Pb$: C, 34.01; H, 3.21; N, 1.65%. Found: C, 34.27; H, 3.00; N, 1.88%. ESI MS calcd for $[C_{24}H_{27}NO_7Pb](ClO_4)^+$: 748.1; Found: 748.1.

1,8-Oxybis(ethyleneoxyethyleneoxy)-10-hydro-10-*N*-acryliminol-anthracene-9-one perchlorate Monohydrate (9). A 0.10 g quantity of **2**, 5.0 mL acrylonitrile, and 0.4 mL of 70% perchloric acid were allowed to stir for 1 h. Both clear, block crystals and an amorphous white powder were isolated after sitting overnight. Overall yield = 0.12 g (87%). Clear, block crystals have a melting point = 195−205 C (dec) and include a water of hydration. Elemental analyses calcd for $C_{25}H_{28}ClNO_{11}.H_2O$: C, 52.49; H, 5.29; N, 2.45%. Found: C, 52.30; H, 5.13; N, 2.61%. ESI MS calcd for M^+: 454.5; Found: 454.1. ^{1}H NMR (CD_3CN at 22 °C): δ 3.50−4.30 (*m*, 16H, -OCH_2 from polyether chain); 6.10 (*dd*, 6.6 Hz, 1H, -CH=); 6.31 (*t*, 4.4 Hz, 2H, =CH_2); 6.64 (*d*, 9.4 Hz, 1H, methine); 7.06 (*d*, 8.2 Hz, 2H, ArH); 7.30 (*t*, 8.2 Hz, 2H, ArH); 7.86 (*d*, 7.8 Hz, 2H, ArH); 8.59 (*d*, 9.4 Hz, 1H, NH). ^{13}C NMR (CD_3CN and three drops of d^3-DMSO at 22 °C): δ 68.1; 68.7; 69.6 69.7; 115.6; 117.7; 125.2; 128.3; 129.3; 132.2; 133.9; 155.5; 163.1; 182.3.

1,8-Oxybis(ethyleneoxyethyleneoxy)-10-hydro-10-*N*-acryliminol-anthracene-9-one perchlorate dichloromethane (10). Crystals grown from amorphous **7** dissolved in CH_2Cl_2:MeOH (8:2) and diffused with diethyl ether produced the dichloromethane solvate in quantitative yield. The melting point = 155−160 C (dec). Elemental analyses calcd for $C_{25}H_{28}ClNO_{11}\cdot 0.9CH_2Cl_2$: C, 49.35; H, 4.76; N, 2.22%. Found: C, 49.74; H, 4.64; N, 2.47%. The proton NMR is identical to **7**.

1,8-Oxybis(ethyleneoxyethyleneoxy)-10-hydro-10-N-acryliminol-anthracene-9-one perchlorate acetonitrile (11). Recrystallization of **7** from acetonitrile-diethyl ether produces the acetonitrile solvate. Melting point = 150−154 C (dec), $C_{25}H_{28}ClNO_{11}\cdot CH_3CN$: C, 54.50; H, 5.25; N, 4.71%. Found: C, 54.17; H, 5.09; N, 4.71%. The proton NMR is identical to **7**.

1,8-Oxybis(ethyleneoxyethyleneoxy)-10-hydro-10-*N*-heptiminol-anthracene-9-one perchlorate (12). A 0.20 g quantity (0.50 mmol) of **2** in 5.0 mL of *n*-heptylcyanide were combined in a similar manner as **3**. A pale yellow solid was obtained, filtered, washed several times with diethyl ether, and dissolved in methylene chloride: methanol (8:2) and diffused with diethyl ether. Pale yellow colored crystals were obtained. Yield: 0.14 g (45%) and the melting point = 142−145 °C (dec). Elemental analyses calcd for $C_{30}H_{40}ClNO_{11}$: C, 57.55; H, 6.44; N, 2.24%. Found: C, 57.57; H, 6.21; N, 2.18%. ESI MS calcd for M^+: 526.5; Found: 525.8. ^{1}H NMR (CD_3CN at 22 °C): δ 0.76−1.58 (*m*, 13H, CH_3 and -CH_2 from alkyl chain); 2.50 (*t*, 7.4 Hz, 2H, -CH_2C=O); 3.64−4.27 (*m*, 16H, -OCH_2); 6.61 (*d*, 9.4 Hz, 1H, methine H); 7.28 (*d*, 8.2 Hz, 2H, ArH); 7.58 (*t*, 8.2 Hz, 2H, ArH); 7.84 (*d*, 7.8 Hz, 2H, ArH); 8.26 (*d*, 9.4 Hz, 1H, NH). ^{13}C NMR (CD_3CN at 22 °C): δ 14.3; 23.1; 24.7; 28.9; 29.1; 32.2; 34.1; 42.9; 68.7; 69.7; 70.8; 71.3; 125.8; 131.5; 133.6; 157.8; 179.8.

1,8-Oxybis(ethyleneoxyethyleneoxy)-10-*N*-(4-cyano)butiminol-10-hydro-anthracene-9-one perchlorate (13). A 0.20 g quantity (0.50 mmol) of **2** in 5 mL of 1,4-dicyanobutane was mixed with 0.5 mL of 70% perchloric acid and the solution stirred. Toluene was added, and the precipitate was filtered and washed with diethyl ether. The solid was dissolved in acetonitrile/methanol (8:2) mixture and diffused with diethyl ether. Lemon yellow-colored crystals were obtained. Yield: 0.10 g (33%) and the melting point = 165−68 °C (dec). Elemental analyses calcd for $C_{28}H_{33}ClN_2O_{11}$: C, 55.22; H, 5.46; N, 4.60%. Found: C, 54.29; H, 5.35; N, 4.78%. ESI MS calcd for M^+: 509.58; Found: 509.32. ^{1}H NMR (CD_3CN at 22 °C): δ 1.39−1.72 (*m*, 4H, CH_2); 2.31 (*t*, 2H, CH_2); 2.54 (*t*, 2H, CH_2); 3.61−4.25 (*m*, 16H, -OCH_2); 6.63 (*d*, 9.0 Hz, 1H, methine H); 7.31 (*d*, 8.2 Hz, 2H, ArH); 7.60 (*t*, 8.2 Hz, 2H, ArH); 7.86 (*d*, 7.8 Hz, 2H, ArH); 8.29 (*d*, 9.0 Hz, 1H, NH).

1,8-Oxybis(ethyleneoxyethyleneoxy)-10-*N*-(5-norbornenyl-2-iminol)-10-hydro-anthracene-9-one perchlorate (14). A 0.15 g quantity of **2**, 1.1 equiv (0.057 g) of 5-norbornene-2-carboxamide, and 7 mL of benzonitrile were allowed to stir for 5 min. Several drops of 70% perchloric acid were added to the mixture and stirred for 30 min. The solution was diffused with ether overnight and clear, amber, needle-like crystals were isolated. Overall yield = 0.14 g (61%). Elemental analyses calcd for $C_{30}H_{34}ClNO_{11}$: C, 58.11; H, 5.53; N, 2.26%. Found: C, 58.31; H, 5.45; N, 2.62%. ESI MS calcd for M^+: 519.59; Found: 519.9. ^{1}H NMR 500 MHz (CD_3CN at 22 °C): δ 1.01 (*m*, 1H, norb. CH_2); 1.45 (*m*, 2H, norb. CH_2); 2.06 (*m*, 1H, norb. CH_2); 2.94 (*s*, 1H, norb. CH); 3.25 (*m*, 1H, C(O)CH-); 3.70 (*s*, 1H, norb. CH); 3.70−4.40 (*m*, 16H, -OCH_2); 6.62 (*d*, 8.5 Hz, 1H, anthracenone CH); 6.12 (*dd*, 1H, =CH); 5.46 (*dd*, 1H, =CH); 7.35 (*d*, 8.2 Hz, 2H, ArH); 7.63 (*t*, 8.2 Hz, 2H, ArH); 7.63 (1H, NH); 7.88 (*d*, 7.8 Hz, 2H, ArH).

1,8-Oxybis(ethyleneoxyethyleneoxy)-10-*N*-(5-norbornenyl-2-amido)-10-hydro-anthracene-9-one (15). 14 was neutralized in a manner similar to **5** in quantitative yield. Melting point = 210−214 °C (dec). Elemental analyses calcd for $C_{30}H_{33}NO_7\cdot H_2O$: C, 67.03; H, 6.56; N, 2.60%. Found: C, 66.98; H, 6.48; N, 2.46%. ^{1}H NMR ($CDCl_3$ at 22 °C): δ 1.15 (*m*, 1H, norb. CH_2); 1.25 (*m*, 2H, norb. CH_2); 1.52 (*m*, 1H, norb. CH_2); 2.64 (*m*, 1H, C(O)CH-); 2.70 (*s*, 1H, norb. CH); 3.23 (*s*, 1H, norb. CH); 3.70−4.28 (*m*, 16H, -OCH_2); 5.28 (*dd*, 1H, =CH); 5.80 (*d*, 6.6 Hz, 1H, anthracenone CH); 5.95 (*dd*, 1H, =CH); 7.08 (*d*, 8.2 Hz, 2H, ArH); 7.37 (*t*, 8.2 Hz, 2H, ArH); 8.29 (*d*, 6.6 Hz, 1H, NH); 7.88 (*d*, 7.8 Hz, 2H, ArH). Crystals were grown from 9:1 methylene chloride/methanol mixture and diffused with diethyl ether.

NMR. ^{1}H, COSY (Correlation Spectroscopy) and 1D-NOESY (Nuclear Overhauser Effect Spectroscopy) NMR experiments were recorded on a Varian INOVA 500 spectrometer fitted with an Inverse Detection Probe and Pulsed Field Gradient Driver, at 23 °C, operating at 500 MHz. Specifically, for the 1D-NOESY experiments a relaxation delay of 1 s, a mixing time of 350 ms, and an acquisition time of 1.998 s were employed. Chemical shifts were referenced to the appropriate residual protonated solvent peaks.

Crystallography. Crystallographic data were collected using Mo Kα radiation on a Bruker SMART APEXII CCD diffractometer. Cell constants were calculated from greater than ~9,000 reflections. Date reduction and refinement were completed using SHELXTL and the WinGX suite of crystallographic software.[18,19] Structures were solved using SIR92.[20] All hydrogen atoms, except the amide H(98) and oxonium H(99) atoms, were placed in ideal positions and refined as riding atoms with relative isotropic displacement parameters. Positions of amide and oxonium hydrogen atoms were determined from residual electron density in the difference maps. Table 1 lists additional crystallographic and refinement information.

(18) *SHELXTL-Plus*; Bruker Analytical X-ray Systems: Madison, WI, 2006.
(19) Farrugia, L. J. *J. Appl. Crystallogr.* **1999**, *32*, 837.
(20) Altomare, A.; Burla, M. C.; Camalli, M.; Cascarano, G.; Giacovazzo, C.; Guagliardi, A.; Moliterni, A. G. G.; Polidori, G.; Spagna, R. *J. Appl. Crystallogr.* **1998**, *32*, 115–119.

Table 1. Crystallographic and Refinement Data for Neutral Amide and Protonated/Metalated Iminol Adducts of Compound **2**

	3	**4**	**5**	**7**	**15**	**8**	**9**	**10**	**11**
R Group	methyl	ethyl	ethyl (deprotonated)	phenyl (deprotonated)	norbornenyl (deprotonated)	[3·Pb](ClO$_4$)$_2$	acrylo (H_2O)	acrylo (CH_2Cl_2)	acrylo (ACN)
empirical formula	$C_{24}H_{28}ClNO_{11}$	$C_{25}H_{30}ClNO_{11}$	$C_{25}H_{29}NO_7$	$C_{29}H_{29}NO_7$	$C_{30}H_{33}NO_7$	$C_{24}H_{27}Cl_2NO_{15}Pb$	$C_{25}H_{30}ClNO_{12}$	$C_{26}H_{30}Cl_3NO_{11}$	$C_{27}H_{31}ClN_2O_{11}$
formula weight	541.92	555.95	473.51	503.53	519.57	847.60	571.95	638.86	594.99
temperature, K	100(2)	100(2)	100(2)	100(2)	100(2)	100(2)	125(2)	125(2)	125(2)
crystal system	triclinic	triclinic	orthorhombic	monoclinic	triclinic	monoclinic	monoclinic	triclinic	monoclinic
space group	$P\bar{1}$	$P\bar{1}$	$P212121$	$P21/c$	$P\bar{1}$	$P21/c$	$P21/n$	$P\bar{1}$	$P21/n$
a, Å	8.9158(1)	8.352(1)	7.912(4)	13.0944(7)	9.6314(17)	11.6983(7)	11.4132(6)	10.0567(4)	13.1504(8)
b, Å	11.8831(2)	10.933(1)	13.222(6)	13.4476(7)	17.223(3)	14.9918(9)	17.8022(9)	11.4232(4)	14.9570(9)
c, Å	11.9370(2)	15.163(2)	22.398(11)	14.3000(8)	25.030(6)	16.0738(10)	13.2483(7)	12.0954(5)	14.6703(8
α, deg	96.650(1)	107.619(2)			104.345(3)			87.03	
β, deg	91.421(1)	92.281(2)		100.9390(10)	93.238(3)	102.028(1)	107.562(1)	84.92	109.7390(10)
γ, deg	107.366(1)	98.963(2)			105.859(2)			87.69	
volume, Å^3	1196.6(1)	1298.1(3)	2343(2)	2472.3(2)	3834.9(1)	2757.1(3)	2566.3(2)	1381.3(1)	2716.0(3)
Z	2	2	4	4	6	4	4	2	4
density (calc) g cm^{-3}	1.504	1.422	1.342	1.353	1.350	2.042	1.480	1.536	1.455
absorb. coef. mm^{-1}	0.225	0.210	0.100	0.097	0.096	6.392	0.217	0.395	0.207
F(000)	568	582	1008	1064	1656	1656	1200	664	1248
θ range	1.0−25.05	1.0−25.05	1.0−25.05	1.58−25.00	1.00−25.00	1.00−25.00	2.29−25.38	1.0−25.36	1.0−25.36
index ranges, hkl	±10,14,14	±9,13,18	±9,15,26	±15,15,17	±11,19,29	±13,21,21	±13,21,21	±12,13,14	±15,18,17
reflections measured	14685	12013	23063	23904	13489	26345	25444	14010	26876
unique reflections	4232	4560	4158	4360	9917	4853	4716	5049	4963
min/max trans.	0.915/0.978	0.908/0.979	0.930/0.987	0.959/0.985	0.972/0.991	0.179/0.567	0.829/0.914	0.821/0.894	0.836/0.988
data/restr./param.	3349/0/343	3357/0/347	4019/0/320	3285/0/338	9917/3/1039	4000/0/392	4358/0/368	4401/0/385	4003/0/379
goodness-of-fit	1.023	1.029	1.052	1.048	1.075	1.042	1.042	1.054	1.046
final R indices [$I > 2\sigma(I)$]	0.0354	0.0552	0.0261	0.0404	0.1071	0.0242	0.0279	0.0696	0.0440
R indices (all data)	0.0814	0.1481	0.0667	0.0959	0.2943	0.0576	0.0749	0.2063	0.1146
peak/hole	0.44/−0.42	0.97/−0.55	0.14/−0.16	0.51/−0.21	1.45/−1.05	1.53/−0.71	0.24/−0.51	1.11/−1.12	0.35/−0.45
CCDC Number	672238	672243	672244	699701	704545	686946	672241	672239	672240

Scheme 3. Ritter Amide Synthesis

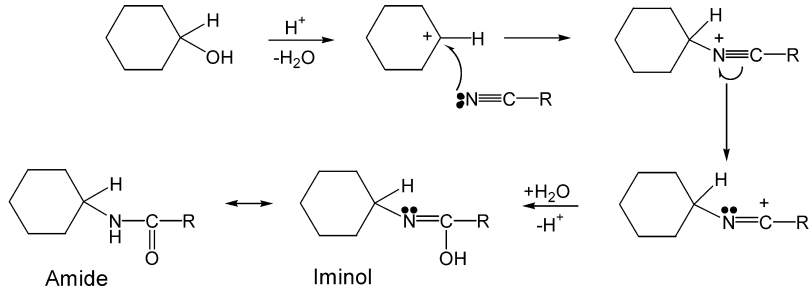

Results

Taking advantage of the rich reduction chemistry of anthraquinone, we have selectively reduced the intraannular carbonyl in **1** to yield the secondary alcohol, **2**, in high yield (Scheme 2).[21] Because the chemical shifts of the aromatic protons in **2** remain almost the same as in **1**, and because of the resulting chemistry of compound **2** (vide infra), only the carbonyl group contained within the polyether ring is reduced. Reaction of secondary alcohols with nitriles under acidic conditions produces corresponding amides (the Ritter amide synthesis).[15,16] The mechanism of the Ritter amide synthesis is outlined in Scheme 3.[22] The secondary alcohol is first protonated by strong acid and loses water to form a carbocation. Reaction with the nucleophilic nitrogen on the nitrile eventually generates another carbocation that is attacked by water to yield the iminol which subsequently tautomerizes to form the amide.

Using a series of nitriles (Scheme 2), the synthesis of several unique amide derivatives, including both saturated (methyl (**3**), ethyl (**4**), heptyl (**12**)) and unsaturated functionalities (acrylo (**9**−**11**), and adipo (**13**)), have been made and characterized. Addition of at minimum 2−3 drops of 70% perchloric acid to compound **2** dissolved in neat nitriles initially produces a blue solution, ascribed to production of the carbocation, that rapidly fades to yellow. Upon standing, typically overnight, X-ray quality crystals of the resulting amides are isolated in ∼50% yield, or the compounds may be isolated by precipitation using a nonpolar solvent and crystals grown by vapor diffusion. All of the adducts have been well characterized by mass spectrometry, proton and carbon NMR, and elemental analyses in addition to single crystal X-ray crystallography. The stability of all the acid adducts is significant as well, where solids melt, with decomposition, at temperatures ranging from ∼148−170 °C.

The phenyl amide derivative, **6**, cannot be made by this method, however. Because of resonance contributions of the aromatic ring, benzonitrile is unreactive in the presence of **2** and perchloric acid. However, benzamide ($C_6H_5C(O)NH_2$), the hydrolyzed benzonitrile, reacts readily and forms the protonated iminol derivative **6** when combined with **2**. In

(21) Criswell, T. R.; Klanderman, B. H. *J. Org. Chem.* **1974**, *39*, 770–774.

(22) (a) Olah, G. A.; Wang, Q. *Synthesis* **1992**, *11*, 1090. (b) Colombo, M. I.; Bohn, M. L.; Ruveda, E. A. *J. Chem. Educ.* **2002**, *79*, 484. (c) Gerasimova, N. P.; Nozhnin, N. A.; Ermolaeva, V. V.; Ovchinnikova, A. V.; Moskvichev, Y. A.; Alov, E. M.; Danilova, A. S. *Mendeleev Commun.* **2003**, *13*, 82.

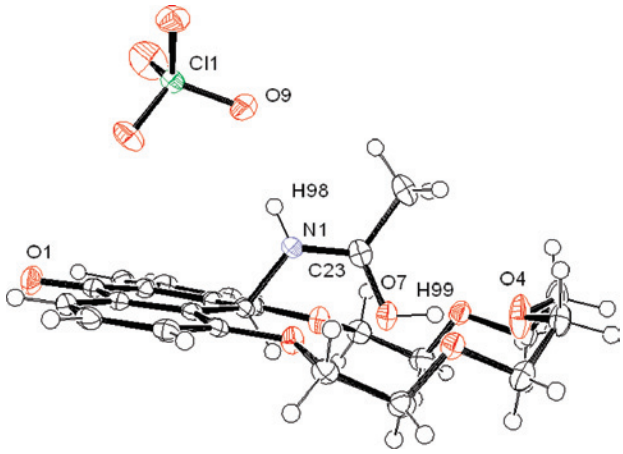

Figure 1. Thermal ellipsoid diagram (50%) of **3**: [**2**-$NH(CH_3)COH]ClO_4$.

fact, because of its unreactivity, we have employed benzonitrile as the solvent for reactions involving primary amides. The synthesis of the norbornene derivative **14** was also produced via reaction of the primary amide, 5-norbornene-2-carboxamide. Reaction of commercial 5-norbornene-2-nitrile, a 50:50 endo/exo mixture did not yield a crystalline product. Reaction of **2** with 5-norbornene-2-carboxamide (80:20 endo/exo ratio) did yield exclusively the endo isomer of the protonated acid upon crystallization. Transformation of primary amides to secondary amides has previously been documented.[23]

X-ray crystallography confirms that protonated iminols rather than amides are produced in all cases, where the amide oxygen is found protonated by the catalytic mineral acid used in the synthesis. This produces an oxonium-based solid acid that is stabilized by an intramolecular hydrogen bond that has not been previously observed. The O−H···O hydrogen bond that forms always occurs between the protonated amide oxygen and the central ether oxygen of the encapsulating polyether ring. Crystal structures of all structures have been similarly labeled to provide close comparison of different nitrile adducts. As shown in Figure 1, the amide/iminol nitrogen = N(1), the amide/iminol carbon = C(23), the amide/iminol oxygen = O(7), the central polyether oxygen = O(4), the remaining anthracenone carbonyl oxygen = O(1), and the hydrogen-bonded perchlorate oxygen = O(9). H(98), attached to N(1), is referred to as the amide proton, and the position of H(98) and the oxonium proton (H99) have all been determined from residual electron density and have not been placed in idealized positions as riding atoms in all structures. Hydrogen bond distances and bond angles and other important bond distances specific to each structure are reported in Table 2.

In eight related structures, compounds **3**, **4**, **9**-**14**, the O-protonated amide adducts, the "closed" form of the latch, have been characterized. The hydrogen bond distance between the protonated amide oxygen O(7) and the polyether oxygen O(4) averages 2.573 ± 0.045 Å with bond angles

(23) (a) Cheeseman, G. W. H.; Poller, R. C. *J. Chem. Soc.* **1962**, 5277. (b) Motokura, K.; Nakagiri, N.; Mizugaki, T.; Ebitani, K.; Kaneda, K. *J. Org. Chem.* **2007**, *72*, 6006.

Table 2. Hydrogen Bond Distances (Å) and Angles (deg) between Heavy Atoms and Other Significant Bond Distances and Angles

	3 Methyl	4 Ethyl	5 Ethyl deprotonated	7 Phenyl deprotonated	15 Norbornenyl deprotonated	12 Heptyl	13 Adipo	14 Norbornenyl	9 Acrylo (H_2O)	10 Acrylo (CH_2Cl_2)	11 Acrylo (ACN)
figure #	1	2	3	4	4	S1	S2	S3	7	8	8
$O(7)_{amide}-H(99)\cdots O(4)_{ether}$	2.530(2), 178(3)	2.647(3), 170(5)				2.567(2), 172(2)	2.522(2), 172(2)	2.571(2) 166(2)		2.577(3), 166(3)	2.593(2), 164(3)
$O(7)_{amide}-H(99)\cdots O_{H2O}$			2.793(2), 176(2)						2.413(2), 165(2)		
$O_{H2O}-H\cdots O_{ether\ or\ amide}$			3.063(2), 167(2)						2.672(2), 174.4(2)		
									2.717(2), 174(2)		
$N(1)_{amide}-H(98)\cdots O(9)_{perchlorate}$	2.875(2), 174(2)								2.904(3), 159.0(1)	2.825(5), 166(3)	3.057(3), 147(2)
											3.185(3), 154(2)
$N(1)_{amide}-H(98)\cdots O(1)_{carbonyl}$		2.845(4), 160(3)				2.894(2), 153(2)	2.862(2) 158(2)	2.847(3) 158(2)			
$N(1)_{amide}-H(98)\cdots O_{H2O}$			2.894(2), 177(2)								
$C(23)-O(7)-O(4)$	113.9	114.2				116.2	117.1	123.6		119.1	124.2
$C(23)-O(7)-O(8)$									133.3		
$C(6)=O(1)_{quinone}$	1.226(2)	1.251(4)	1.227(2)	1.224(2)	1.238(5)	1.229(2)	1.229(2)	1.233(3)	1.223(2)	1.219(4)	1.232(3)
$C(23)=O(7)_{amide}$	1.283(2)	1.325(4)	1.236(2)	1.232(2)	1.229(5)	1.290(2)	1.291(2)	1.292(3)	1.271(2)	1.282(4)	1.289(2)
$C(23)-N(1)_{amide}$	1.301(2)	1.319(4)	1.339(2)	1.343(2)	1.342(5)	1.297(2)	1.298(2)	1.301(4)	1.316(2)	1.302(4)	1.304(3)
C=C									1.322(2)	1.245(6)	1.242(4)
C'N							1.145(2)				
anthracenone plane, dihedral angle	173.5	179.3	159.1	172.9	174.3	180.0	179.1	180.0	164.5	172.5	164.1
melting point (C, dec.)	148−150	168−171	268−270	228−232	210−214	148−152	165−68		195−205	155−160	150−154

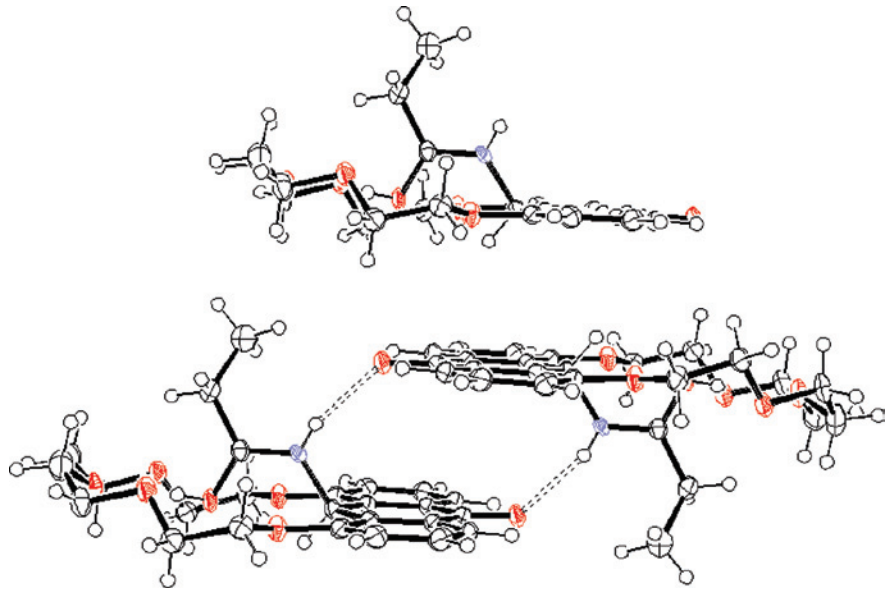

Figure 2. Thermal ellipsoid diagram (50%) of compound **4**: [**2**-NHC(CH_2CH_3)OH]ClO_4. Packing shows formation of N1−H98···O1 hydrogen bond dimers and the pi-stack within and between the dimers. The perchlorate anions are not involved in hydrogen bonding and are omitted for clarity.

averaging 170.0 ± 5.0 degrees, showing that relatively strong hydrogen bonds are indeed formed. The structure of the acetonitrile adduct is shown in Figure 1, where the perchlorate anion is also found hydrogen bonded to the amide proton. According to Boks, *unprotonated* amides have an average N−C amide bond of 1.331 Å and an average C═O bond distance of 1.230 Å.[24] Comparing all the protonated amides above, the amide N−C bond contracts on average to 1.304 ± 0.008 Å and the carbonyl oxygen considerably lengthens to 1.293 ± 0.016 Å. These data are consistent with the amides adopting significant iminol character when the amide carbonyl oxygen has been protonated. Figure 2, the protonated ethyl amide adduct includes crystal packing data discussed later.

Reaction of the protonated ethyl adduct **4** with aqueous base followed by extraction into organic solvent produces a much different deprotonated "open" amide, **5**, as shown in Figure 3, where the free amide adopts a large amplitude change in geometry. Recrystallization from CH_2Cl_2/MeOH generates the monohydrate where water is found hydrogen bonded to the amide oxygen, O(8)−H(8a)···O(7) = 2.793(2) Å, 176(2)°. Here the amide is rotated 180° away from the configuration found in the protonated structures. Now the amide proton, H(98), points toward the center of the ring, and the amide carbonyl is pointing outward forming a hydrogen bond with the water molecule. The amide bond distances, N(1)−C(23) and C(23)−O(7), also match average values for an unprotonated amide.

This same 180 degree change in configuration has also been observed in two separate examples: the deprotonated phenyl derivative, **7**, and the deprotonated norbornene derivative, **15** (Figure 4). The neutral amides are found with normal bond distances, and there are no classic hydrogen bonds found in these structures; the amide proton, H(98), is

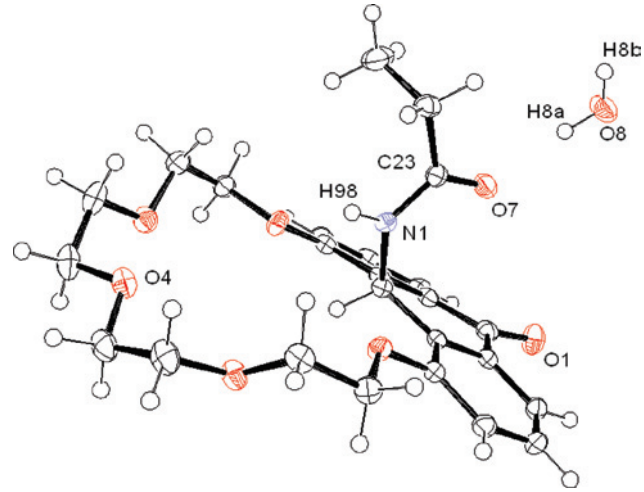

Figure 3. Thermal ellipsoid diagram (50%) of **5**: **2**-NHC(O)CH_2CH_3.H_2O.

almost completely enclosed by the encircling polyethylene rings, with the shortest N(1)−H···O(5) interaction being over 3.8 Å long. These structures demonstrate that the water of hydration, observed previously in the structure of **5**, is unnecessary for an unprotonated derivative to adopt the open configuration.

As shown in Scheme 1, the switch can again be closed by the addition of metal cations that form coordinate-covalent bonds within the macrocycle. The crystal structure of the 1:1 $Pb(ClO_4)_2$/base-neutralized adduct of compound **3** is shown in Figure 5. The Pb(II) cation coordinates to the amide carbonyl oxygen and the three polyether oxygens, closing the switch. The lead cation is large and oxophilic and forms an octa-coordinate, square prismatic complex. One perchlorate anion is found bridging two Pb(II) centers and the second perchlorate chelates with the lead to complete the coordination sphere. The Pb-oxygen bond involving the amide carbonyl oxygen is by far the shortest of the eight Pb−O bonds listed in Figure 4, 2.303(3) Å, and the carbonyl bond

(24) Boks, G. J., Doctoral Thesis, University of Utrecht, The Netherlands, 1997; available under http://www.library.uu.nl/digiarchief/dip/diss/01741627/boks.html.

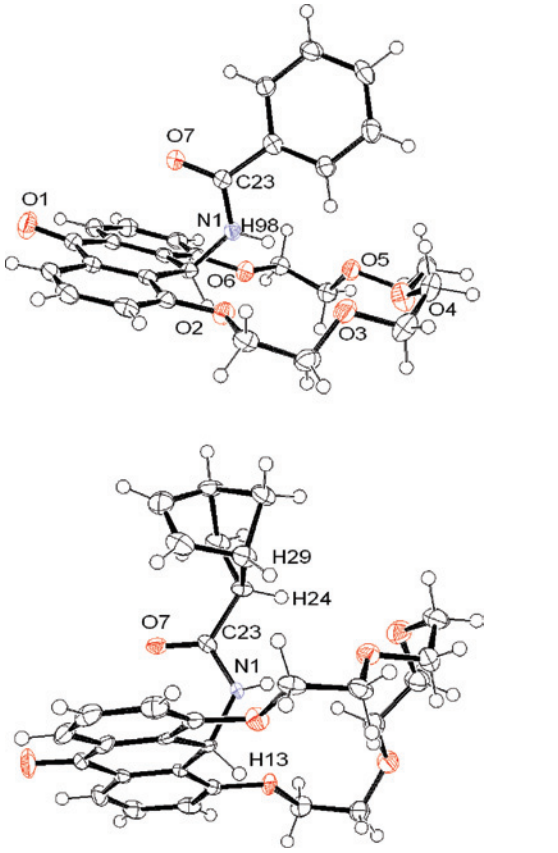

Figure 4. Thermal ellipsoid diagrams (50%) of neutralized amides: (**7**) **2**-NHC(O)(Phenyl) (top) and (**15**) **2**-NHC(O)(norbornene) (bottom).

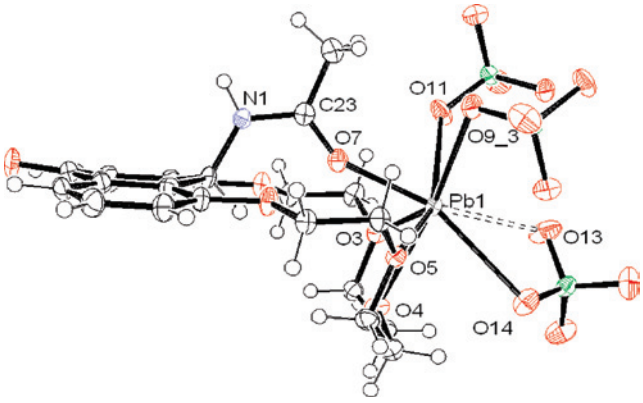

Figure 5. Thermal ellipsoid diagram (50%) of compound **8**: [(**2**-NHC(O)CH_3)Pb]$(ClO_4)_2$. Pb−O(7)$_{amide}$ = 2.303(3), Pb−O(3)$_{ether}$ = 2.640(3), Pb−O(4)$_{ether}$ = 2.528(3), Pb−O(5)$_{ether}$ = 2.626(3), Pb−O(11)$_{ClO4}$ = 2.673(3), Pb−O(9)$_{ClO4}$ = 2.784(3), Pb−O(14)$_{ClO4}$ = 2.889(3), Pb−O(13)$_{ClO4}$ = 3.033(3) Å.

distance, C(23)−O(7) = 1.250(6) Å, is lengthened significantly compared to neutral amides, indicating some iminol character; however, the elongation is not as pronounced as with the protonated adducts. To accommodate the long Pb(II)-oxygen bonds, the polyether chain is bent at approximately a 90° angle from the anthracenone plane. Here the Pb(II) cation is too large to fit entirely within the macrocycle, as was previously observed in the crystal structure of the Pb(II) complex of the anthraquinone starting material, compound **1**.[2d]

Scheme 4

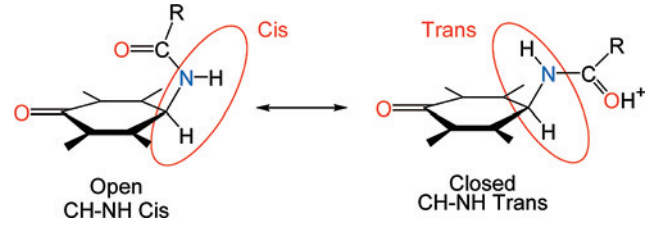

Table 3. Chemical Shift Data and $^3J_{NHCH}$ Coupling Constants of Protonated and Neutralized Amide Products

	-NH		-CH	
compound (#)	δ(ppm)	$^3J_{NHCH}$ (Hz)	δ (ppm)	$^3J_{NHCH}$ (Hz)
		Protonated[a]		
Ethyl (4)	8.23	9.4	6.62	9.4
Phenyl (6)	8.87	9.0	6.70	9.0
Norbornene (14)	∼7.6	*c*	6.62	8.5
		Neutralized[b]		
Ethyl (5)	7.74	7.0	5.77	7.0
Phenyl (7)	8.64	6.2	6.04	7.0
Norbornene (15)	8.29	6.6	5.80	6.6

[a] CD_3CN. [b] $CDCl_3$. [c] Obscured by aromatic resonance.

From the crystallographic studies, the amide peptide bond is always found in the *trans* configuration; however, the CH-NH bond changes between *trans* and *cis* conformations when the latch is open vs closed (Scheme 4). NMR spectroscopy of the protonated ("closed") and deprotonated ("open") adducts found in the solid-state can provide evidence of which conformation is present in solution. Table 3 compares vicinal $^3J_{NHCH}$ coupling constants between the protonated and deprotonated ethyl, phenyl, and norbornene derivatives. From the table, the protonated (closed-*trans*) adducts have, on average, coupling constants that are ∼2 Hz larger than the same deprotonated adducts. This is an indication that the deprotonated adducts maintain the open, *cis* conformation in solution, as the data is consistent with vicinal $^3J_{CHCH}$ coupling constants of alkenes where *trans* coupling constants (∼15 Hz) are also larger than respective *cis* coupling constants (∼8 Hz).

Additional Nuclear Overhauser Effect (NOE) experiments were also performed on both the protonated and deprotonated norbornene adducts, **14** and **15**, to see if through-space interactions could be detected between the anthracenone methine and amide protons. Spectra A and B in Figure 6 are the NOE experiments for the deprotonated norbornene adduct, **15**. Here the through-space interactions are reciprocal between the methine and the amide protons, reinforcing that the unprotonated adduct retains a *cis*-open conformation in solution. In B, other through-space interactions between the amide proton and two of the methine protons (H24 and H29, Figure 4) are also observed. These norbornene methine protons are within 3 Å of the amide proton as measured by crystallography.

For the protonated norbornene adduct, **14**, at 500 MHz, the amide proton overlaps with the resonance of an aromatic proton (Supporting Information, Figure S4). Integration, the 2D COSY (Supporting Information, Figure S5) spectrum, and the disappearance of this resonance (and the resulting loss of coupling to the anthracenone methine proton) when

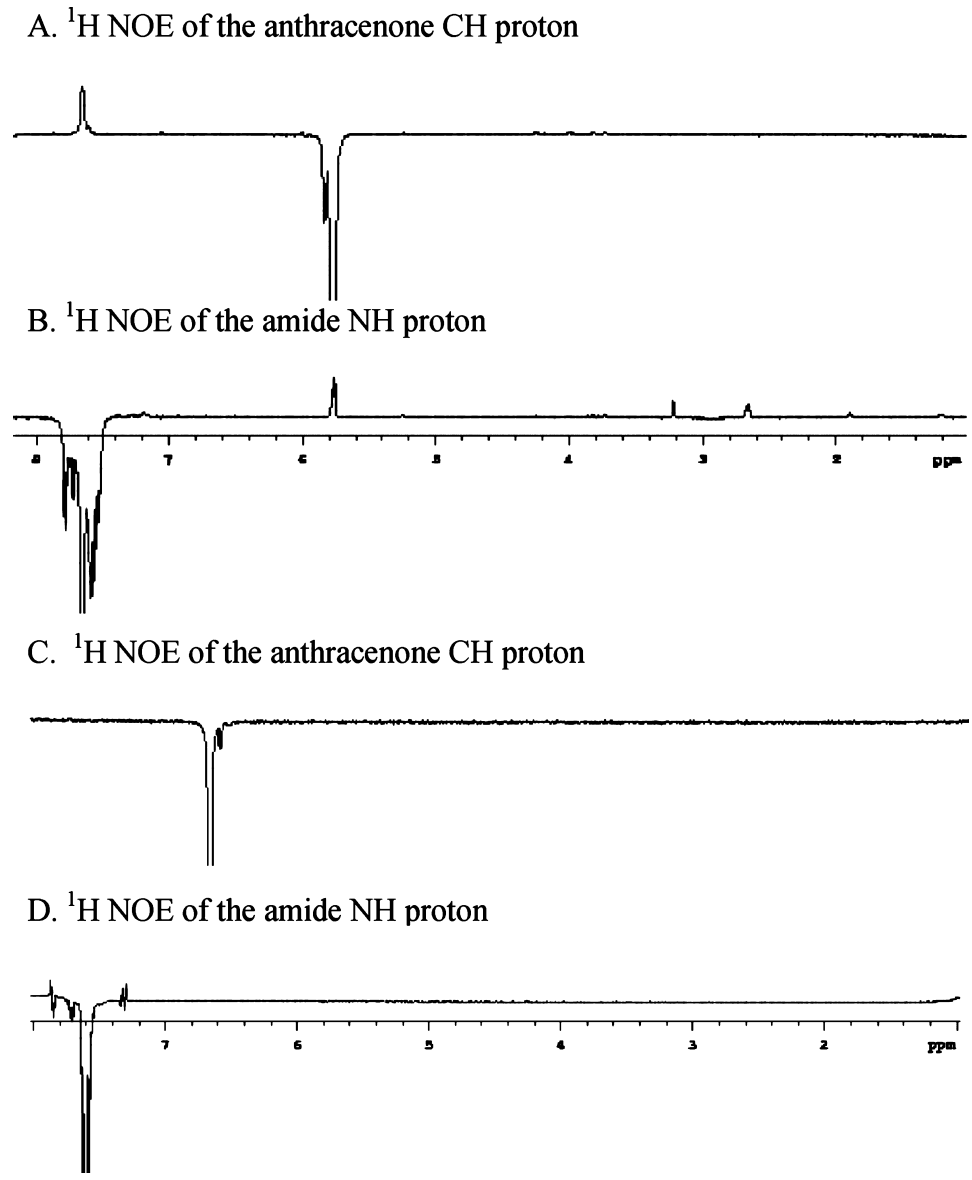

Figure 6. (A, B) ^{1}H NOE spectra of the deprotonated norbornene amide, compound **15**, in $CDCl_3$. (C, D) ^{1}H NOE spectra of the protonated norbornene adduct, compound **14**, in CH_3CN.

mixed with a drop of D_2O indicate the amide proton has a chemical shift of ~7.6 ppm. The NOE experiments of the protonated norbornene adduct in C and D in Figure 6 show no reciprocal through-space interactions whatsoever. Since protonated adducts adopt the *trans* configuration in solution, this is the expected result.

We have attempted to determine the pH conditions where the switching mechanism reverts between open and closed configurations in solution; however, we have been unsuccessful since either or both the protonated or unprotonated adducts are insoluble in MeOH/water or DMSO/water mixtures or produce precipitates upon large pH change. Addition of deuterated HCl to **5** in MeOD/CD_2Cl_2 only confirms that 1 equiv of acid is added at the end point of the NMR titration.

A different type of iminol adduct, **9**, forms after dissolving **2** in neat acrylonitrile and adding concentrated perchloric acid. Clear block crystals of **9** appear along with an amorphous, white precipitate that was recrystallized in either CH_2Cl_2/MeOH mixture or acetonitrile to produce the solvates **10** and **11**, respectively. The thermal ellipsoid diagram of **9** is shown in Figure 7. Most striking in this structure is the presence of a water molecule encapsulated within the macrocycle, hydrogen-bonded to the polyether chain, and accepting a proton from the protonated amide oxygen O(7). The polyether ring is bent at almost a 90° angle to accommodate the water molecule; whereas in previous structures the polyether ring is coplanar with the anthracenone. An extremely short hydrogen bond is observed between the protonated amide oxygen and the water oxygen, O(7)−H(99)···O(8) = 2.413(2) Å, 165(2)°. The hydrogen bonds that form between the water and the polyether oxygens are also shorter than typical water-oxygen hydrogen bonds, O(12)−H(12a)···O(3) = 2.672(2), 174.4(2) and O(12)−H(12b)···O(5) = 2.717(2), 174(2), indicating delocalization of the positive charge from the oxonium ion onto the water. The proton NMR spectrum of this compound also shows over fifty discernible peaks for the sixteen methylene

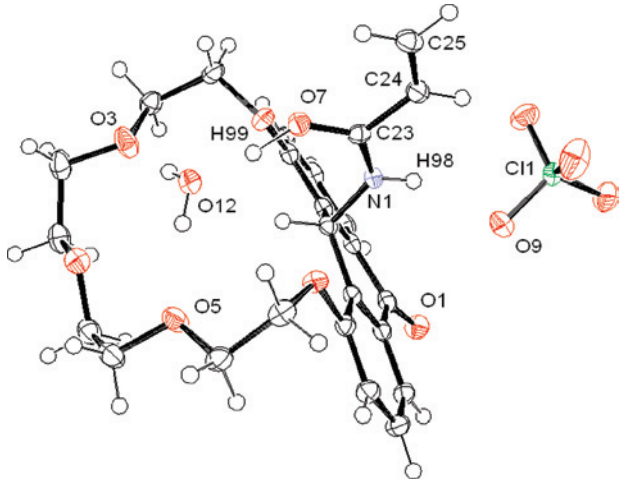

Figure 7. Thermal ellipsoid diagram (50%) of **9**: [**2**-NHC(CH=CH_2)-OH···H_2O]ClO_4.

hydrogens on the polyether ring. A theoretical maximum of 64 peaks is predicted if each side of the polyether ring is equivalent and the ring is conformationally inert. The perchlorate is hydrogen bonded to the amide hydrogen, H(98), in this structure, and the anthracenone plane is significantly bent as well (164.5 °), consistent with previous results.

Two different *intermolecular* hydrogen bonding motifs occur within these structures. For the acetonitrile adduct (Figure 1), the perchlorate counteranion is found hydrogen-bonded to the amide hydrogen H98 (N1−H98···$O(9)_{perchlorate}$ = 2.880(2) Å, 168.1(13)°). In the lattice, two neighbors share a planar, anthracenone face on the side away from the iminol group to form pi-stack *dimers* with a separation of approximately 3.4−3.5 Å. Infinite pi-stacks within the crystal are prevented from forming, however, by the location of the perchlorate which is hydrogen bonded to the amide hydrogen and positioned over the opposite anthracenone face as shown in Figure 1.

The ethyl (**4**), heptyl (**12**), and adiponitrile (**13**) adducts, however, (Figure 2 and Supporting Information, Figures S1, S2) do not pack such that the amide hydrogen, H(98), forms a hydrogen bond with the perchlorate anion. Instead hydrogen bonded *dimers* are formed between pairs of opposing amide nitrogens, N(1), and the carbonyl oxygens, O(1), in neighbors as shown in Figure 2 for the ethyl adduct. Both the pi-stack that forms *within* the dimer and the pi-stack that forms *between* dimers average ∼3.6 Å in separation, producing an infinite pi-stack within the crystal. The anthracenone plane in these three structures is essentially flat (the dihedral angle formed between the two aromatic rings = 179.5 ± 0.5°).

It is tempting to attribute these two different hydrogen bonding motifs to the number and position of carbon atoms in the iminol alkyl group. For the ethyl adduct in Figure 2, the ethyl group is positioned in the proximity to H(98), the amide nitrogen proton, potentially blocking access of the bulky perchlorate anion to the amide hydrogen, but does allow access to the carbonyl oxygen of a narrow anthracenone with concomitant formation of a pi-stack. The same type of steric hindrance would not take place with the acetonitrile adduct, since it lacks the extra carbon atom. We

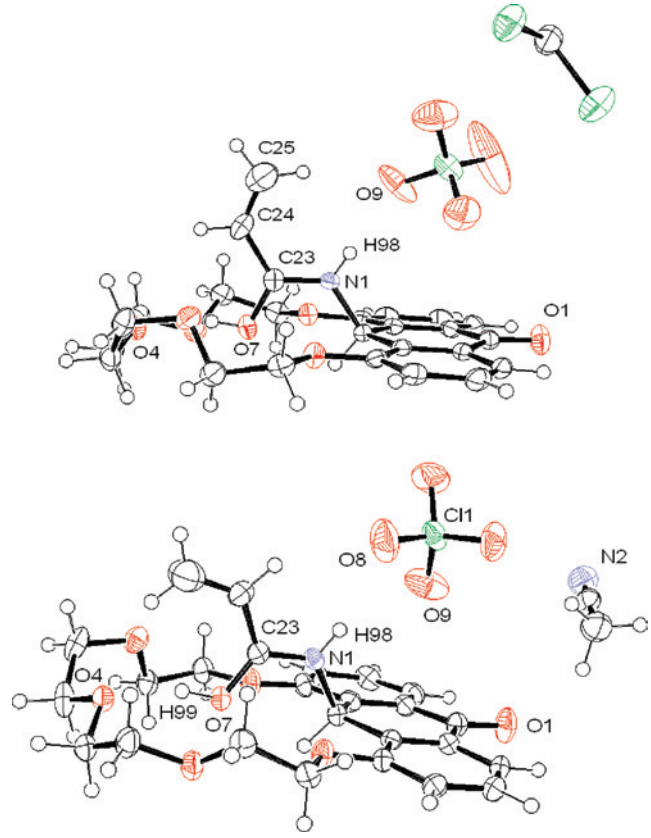

Figure 8. (Top) Thermal ellipsoid diagram (50%) of **10**: [**2**-NHC(CH=CH_2)OH]-ClO_4.CH_2Cl_2. (Bottom) Thermal ellipsoid diagram (50%) of **11**: [**2**-NHC(CH=CH_2)OH]-ClO_4.CH_3CN.

have determined crystal structures of the unsaturated acrylonitrile adduct, however, that disputes this reasoning as shown in Figure 8. The top and bottom crystal structures are dissimilar in that they do contain different solvate molecules in addition to the protonated acrylamido adduct, but also the conformation of the olefin in each case is quite different. For the acetonitrile solvate (bottom), the olefin is rotated away from the amide proton and the perchlorate is found once again hydrogen bonded to the amide (N1−H98··· O9 = 2.825(5) Å), as observed previously for the methyl adduct **3**. In contrast, for the dichloromethane solvate (top), the olefin is found rotated ∼90° into a position almost identical to that found for the saturated ethyl derivative **4** shown in Figure 2; however, the perchlorate is *still* found hydrogen bonded to the amide proton. In this case, the hydrogen bond that forms between the amide and the perchlorate is significantly longer (∼3.0 Å). Adducts where the amide hydrogen H(98) bonds to the anion (**3**, **8**, and **9**) all have a common, bent anthracenone plane (170 ± 5°) and do not form infinite pi-stacks. Overall then, the dihedral angle is an indicator of the type of packing preference that occurs within the crystal. A flat plane maximizes infinite pi-stacking interactions at the expense of hydrogen bonding between the amide hydrogen and the anion. A bent plane implies hydrogen bonding with the anion is more energetically favorable than the energy gained by forming infinite pi-stacks.

Reaction of the secondary alcohol **2** with acid in organic solvents other than nitriles produce only the 10,10′-bian-

throne, where two ring-substituted anthracenones are linked through the central sp^3 hybridized carbon that contains the methine hydrogen. A second molecule of **2** acts as the nucleophile in this case; the nucleophile being most likely the pi electrons of the anthracenediol tautomer. In addition, we have attempted to make protonated amides of open-chain polyether anthracenones without success. Preliminary studies reveal that the corresponding monoalcohol with methoxy groups in the 1 and 8 positions, similar to **2**, also produces a bianthrone, indicating the presence of the macrocyclic ring structure aids in formation and stabilization of these new O-protonated amides.

Discussion

X-ray crystal structures of other protonated carbonyl groups (nonamide related) have been previously reported in the literature, and can be divided into hemiprotonated bridging dimers[25] and protonated carbonyls hydrogen-bonded to the anion,[26] all generated by the addition of the superacids to corresponding ketones. Typically, however, these adducts are stable only at low temperature. The stable protonated oxonium ions we report here are only the second where a protonated carbonyl group has been stabilized by an *intramolecular* hydrogen bond across a macrocycle[13] and the first between an O-protonated amide and an ether oxygen. In earlier work, we reported the hydronium ion adduct of compound **1** which acts as an anion detector because of induced electronic changes in the anthraquinone lumophore.[2a] For [**1**·H_3O]ClO_4, *intramolecular* hydrogen bond distances average 2.570 Å, slightly longer than hydrogen bond distances found in the new solid acids reported here. Short hydrogen bonds of ~2.5 Å are classified as Low-Barrier Hydrogen Bonds (LBHB).[27] Classical hydrogen bonds (~2.8 Å for O−H···O) have a double well potential where the hydrogen is trapped in the deepest well (bonded to the strongest Lewis base). Contraction of the hydrogen bond distance lowers the activation barrier between the two wells and the hydrogen atom position is a mix of tautomeric forms. In these adducts, the acid proton is found bonded to the more basic amide oxygen, O(7), and short hydrogen bonds are attributed to the near ideal geometric match of the protonated amide-ether complex (Scheme 5). The bond angle C(23)−O(7)−O(4) in these structures averages 117.5°, ideal for overlap between lone pairs on the sp^2 hybridized carbonyl oxygen, O(7) and the polyether oxygen, O(4). The hydrogen-bonded lone pair on the ether is also oriented with optimum bond angles only slightly larger than 109.5°.

Scheme 5

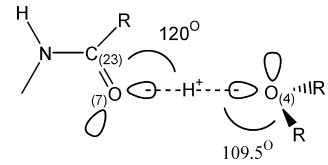

The very short intramolecular 2.413(2) Å hydrogen bond found in **9** is quite exceptional, and compares with other hydrogen bonds observed by direct protonation of diethyl ether and THF using carborane acids ($H(solvent)_2^+$; hydrogen bond distances = 2.40 and 2.37 Å for diethyl ether and THF adducts, respectively).[28] Very short hydrogen bonds have shallow wells or have collapsed completely into a single well, and the hydrogen atom is expected to reside midway between heavy atoms. This is in fact observed in the structure of **9**, where H(99) approaches the midpoint between the protonated amide and the water molecule (O(7)−H(99) = 1.10 A and O(12)−H(99) = 1.35 Å; the sum of these two O−H bonds is larger than the distance between the heavy atoms since the hydrogen bond is slightly bent, 165(2)°).

Conclusions

We have designed new solid acids based upon oxonium ions formed via O-protonation of amides. The intramolecular hydrogen bond that forms between the protonated amide oxygen and the polyether oxygen accounts for the stability of these new oxonium adducts. Stability is apparent from high melting points, the solids are not hygroscopic, and are stable indefinitely in air.

Gain or loss of a proton/metal cation results in a mechanical switch involving large amplitude changes in geometry. The amide group rotates/folds in and out of the macrocycle as *intramolecular* hydrogen bonds or coordinate-covalent bonds are formed/broken as is observed in the "closed" protonated/metal-encapsulated adducts **4** and **6**, and the "open" deprotonated form of compound **5**. Deprotonated adducts maintain the "open" state in solution as observed by NMR.

The latching mechanism, the formation of short, strong LBHB is unique, produced by protonation of a carbonyl group to yield an oxonium ion, which has not been previously employed.

Reduction of the anthraquinone to the secondary alcohol has allowed us to pursue chemistry that adds additional functionality to a macrocyclic polyether ring. As demonstrated, synthetic versatility is possible with the Ritter amide synthesis, but the underlying carbocation chemistry will also allow us to pursue the addition of other nucleophiles.

Acknowledgment. The authors thank NSF-EPSCOR (EPS-0554609) and the South Dakota Governor's 2010 Initiative for financial support and the purchase of a Bruker SMART APEX II CCD diffractometer. A.R.G. was supported by NSF-URC (CHE-0532242) through the

(25) (a) Childs, R. F.; Faggiani, R.; Lock, C. J. L.; Varadarajan, A. *Acta Crystallogr. C* **1984**, *40*, 1291. (b) Esterhuysen, M. W.; Raubenheimer, H. G. *Eur. J. Inorg. Chem.* **2003**, 3861–3869. (c) Wakamiya, A.; Nishinaga, T.; Komatsu, K. *J. Am. Chem. Soc.* **2002**, *124*, 15038–15055.

(26) (a) Montgomery, L. K.; Grendze, M. P.; Huffman, J. C. *J. Am. Chem. Soc.* **1987**, *109*, 4749–4750. (b) Childs, R. F.; Faggiani, R.; Lock, C. J. L.; Mahendran, M.; Zweep, S. D. *J. Am. Chem. Soc.* **1986**, *108*, 1692–1693. (c) Childs, R. F.; Kostyk, M. D.; Lock, C. J. L.; Mahendran, M. *J. Am. Chem. Soc.* **1990**, *112*, 8912–8920. (d) Minkwitz, R.; Schneider, S. *Angew. Chem., Int. Ed.* **1999**, *38*, 714–715.

(27) (a) Perrin, C. L. *Science* **1994**, *266*, 1665–1668. (b) Cleland, W. W.; Kreevoy, M. M. *Science* **1994**, *264*, 1887–1890.

(28) Stasko, D.; Hoffman, S. P.; Kim, K. C.; Fackler, N. L. P.; Larsen, A. S.; Droveyskaya, T.; Tham, F. S.; Reed, C. A.; Rickard, C. E. F.; Boyd, P. D. W.; Stoyanov, E. S. *J. Am. Chem. Soc.* **2002**, *124*, 13869–13876.

Northern Plains Undergraduate Research Center hosted by the University of South Dakota. The LC-ESI-Mass Spec was acquired through NSF-MRI support (CHE-0619190). A.G.S. also thanks ACS-PRF-UFS for additional support.

Supporting Information Available: Thermal ellipsoid diagrams and crystallographic and refinement data for the protonated capronitrile (**11**), adiponitrile (**12**), and nornbornenyl (**14**) adducts, as well as supplemental NMR spectra for compound **15**. Crystallographic files in CIF format for all structures. This material is available free of charge via the Internet at http://pubs.acs.org. X-ray structure data can also be obtained free of charge from the Cambridge Crystallographic Data Center, www.ccdc.cam.ac.uk/conts/retrieving.html.

IC801238A